

NO-A167 611

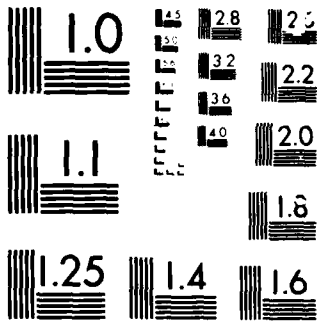
FLOW VISUALIZATION AND VELOCITY MEASUREMENTS IN THE  
SEPARATED REGION OF A. (U) DAVID H TAYLOR NAVAL SHIP  
RESEARCH AND DEVELOPMENT CENTER BET. S C DICKINSON  
MAR 86 DTNSRDC-86/020 F/G 20/4

1/1

UNCLASSIFIED

NL





MICROCOPY

CHART

AD-A167 611

DTNSRDC-86/020

# DAVID W. TAYLOR NAVAL SHIP RESEARCH AND DEVELOPMENT CENTER

Bethesda, Maryland 20884-5000



## FLOW VISUALIZATION AND VELOCITY MEASUREMENTS IN THE SEPARATED REGION OF AN APPENDAGE- FLAT PLATE JUNCTION

by

Stuart C. Dickinson

APPROVED FOR PUBLIC RELEASE; DISTRIBUTION IS UNLIMITED.

Presented at the  
Ninth Symposium on Turbulence  
University of Missouri-Rolla  
Rolla, Missouri  
1-3 October 1984

**DTIC**  
**ELECT**  
MAY 01 1986  
**S**  
**E**

DTIC FILE COPY

SHIP PERFORMANCE DEPARTMENT  
RESEARCH AND DEVELOPMENT REPORT

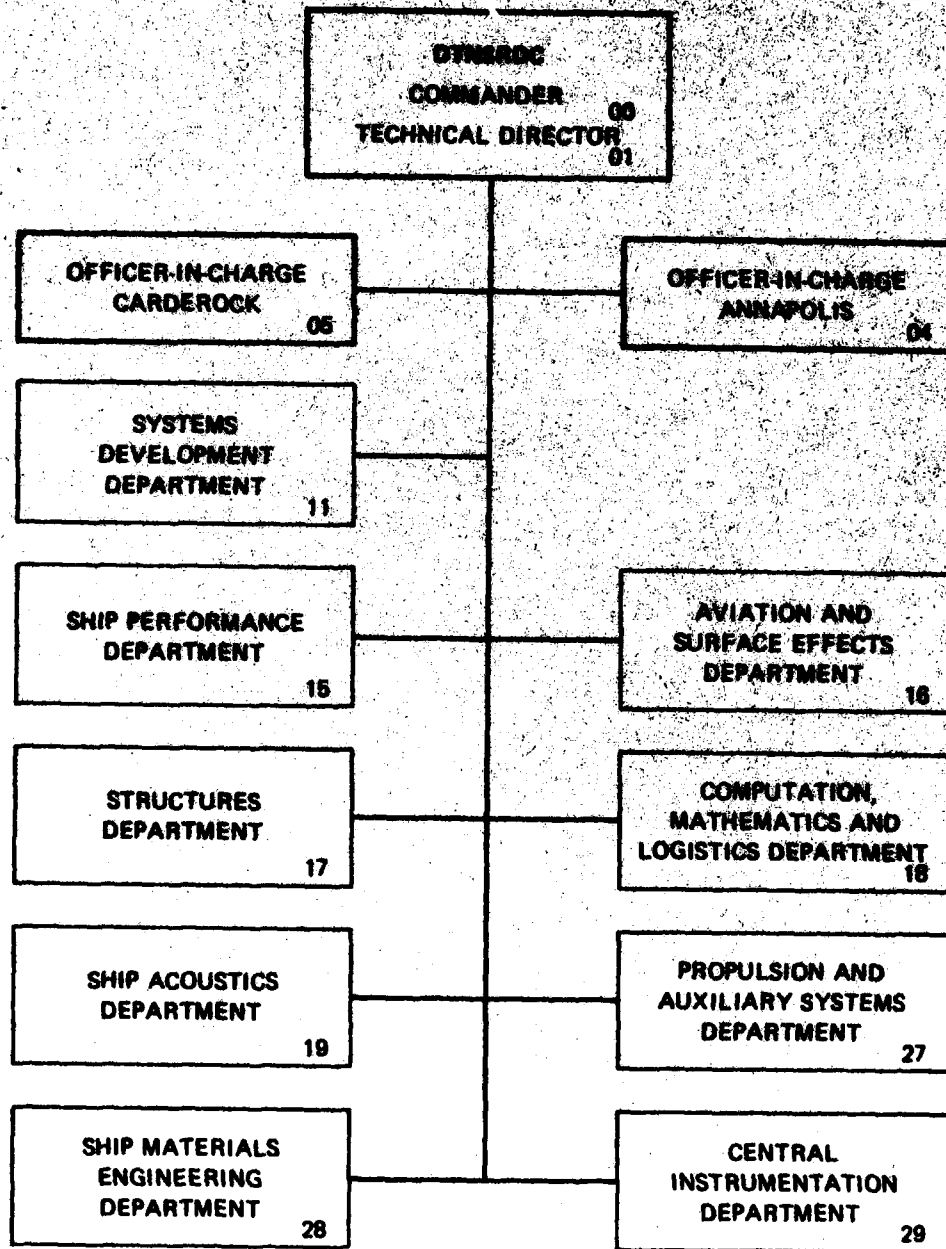
March 1986

DTNSRDC-86/020

FLOW VISUALIZATION AND VELOCITY MEASUREMENTS IN THE SEPARATED  
REGION OF AN APPENDAGE-FLAT PLATE JUNCTION

86 4 30 025

**MAJOR DTNSRDC ORGANIZATIONAL COMPONENTS**



UNCLASSIFIED

SECURITY CLASSIFICATION OF THIS PAGE

ADA 167611

## REPORT DOCUMENTATION PAGE

1a REPORT SECURITY CLASSIFICATION UNCLASSIFIED		1b RESTRICTIVE MARKINGS	
2a SECURITY CLASSIFICATION AUTHORITY		3 DISTRIBUTION/AVAILABILITY OF REPORT APPROVED FOR PUBLIC RELEASE; DISTRIBUTION IS UNLIMITED.	
2b DECLASSIFICATION/DOWNGRADING SCHEDULE		5 MONITORING ORGANIZATION REPORT NUMBER(S)	
4 PERFORMING ORGANIZATION REPORT NUMBER(S)		7a NAME OF MONITORING ORGANIZATION	
6a NAME OF PERFORMING ORGANIZATION David W. Taylor Naval Ship R&D Center	6b OFFICE SYMBOL (if applicable) Code 1542	7b ADDRESS (City, State, and ZIP Code)	
6c ADDRESS (City, State, and ZIP Code) Bethesda, Maryland 20084-5000		9 PROCUREMENT INSTRUMENT IDENTIFICATION NUMBER	
8a NAME OF FUNDING SPONSORING ORGANIZATION Naval Sea Systems Command	8b OFFICE SYMBOL (if applicable) Code 05R24	10 SOURCE OF FUNDING NUMBERS	
8c ADDRESS (City, State, and ZIP Code) Washington, D.C. 20062		PROGRAM ELEMENT NO 61153N	PROJECT NO TASK NO SRO 230101 WORK UNIT ACCESSION NO DN 506152
11 TITLE (Include Security Classification) FLOW VISUALIZATION AND VELOCITY MEASUREMENTS IN THE SEPARATED REGION OF AN APPENDAGE-FLAT PLATE JUNCTION			
12 AUTHOR (Last, First, Middle) Dickinson, Stuart C.			
13a TYPE OF REPORT Formal	13b TIME COVERED FROM TO	14 DATE OF REPORT (Year, Month, Day) 1986, March	15 PAGE COUNT 16
16 SUPPLEMENTARY NOTES Presented at the Ninth Symposium on Turbulence University of Missouri-Rolla, Rolla, Missouri, 1-3 October 1984			
17 DESCRIPTORS 20 04		18 SUBJECT TERMS (Continue on reverse if necessary and identify by block number) Separated Flow Turbulence Flow Visualization Three-Dimensional Flow	
19 ABSTRACT (Continue on reverse if necessary and identify by block number) <p>A "root" vortex forms at the junction of a flat plate and an appendage, creating a three-dimensional, separated flow. Time dependent oil film and oil dot visualizations of this turbulent flow have revealed the vortex system and have provided quantitative information on the direction and the magnitude of the shear stress. Two-dimensional LDV-mean velocity measurements were made in the separated flow region around the leading edge of the appendage, and these measurements are compared here with the flow visualization results.</p>			
20 ABSTRACT TYPE AVAILABLE TO THE ABSTRACT <input checked="" type="checkbox"/> UNCLASSIFIED <input type="checkbox"/> SAME AS RPT <input type="checkbox"/> DTIC USERS		21 ABSTRACT SECURITY CLASSIFICATION UNCLASSIFIED	
22a NAME OF RESPONSIBLE INDIVIDUAL Stuart C. Dickinson		22b TELEPHONE (Include Area Code) (202) 227-1324	22c OFFICE SYMBOL Code 1542

## TABLE OF CONTENTS

	Page
LIST OF FIGURES . . . . .	iii
ADMINISTRATIVE INFORMATION . . . . .	iv
ABSTRACT . . . . .	1
INTRODUCTION . . . . .	1
EXPERIMENTAL DESCRIPTION . . . . .	1
FLOW VISUALIZATION . . . . .	2
LDV MEASUREMENTS . . . . .	6
DISCUSSION . . . . .	7
ACKNOWLEDGEMENTS . . . . .	10
REFERENCES . . . . .	10

### LIST OF FIGURES

1. Appendage junction coordinate system and configuration . . . . .	2
2. Static pressure coefficients $P_s(1/2\rho U_\infty^2)$ measured on the flat plate . . . . .	3
3. Oil film flow visualization on the flat plate at time T after air flow is started . . . . .	4
4. Sketch of "completed oil film visualization . . . . .	5
5. Oil dot visualization pattern . . . . .	5
6. Sketch of oil of wintergreen visualization . . . . .	5
7. Photograph of LDV beam configuration . . . . .	7
8. Normalized U and W velocity profiles at X = -6.5 in. . . . .	8
9. Normalized U and W velocity profiles at X = -0.65 in. . . . .	8
10. Normalized U and W velocity profiles at X = 1.0 in. . . . .	8

11. Normalized U and W velocity profiles at X = 6.5 in. . . . . 9

12. Normalized U velocity profiles along the plane of symmetry (Z=0) ahead of the appendage . . . . . 9

ADMINISTRATIVE INFORMATION

The work described in this report was funded under the Naval Sea Systems Command (05R24) Special Focus Program on Ship and Submarine Appendage Drag and Wake Prediction, Program Element 61153N, Task Area SR0230101, and DTNSRDC Work Unit 1542-101.

Accession For	
NTIS GRA&I	<input checked="" type="checkbox"/>
DTIC TAB	<input type="checkbox"/>
Unannounced	<input type="checkbox"/>
Justification	
By _____	
Distribution/	
Availability Codes	
Dist	Avail and/or Special
A-1	

FLOW VISUALIZATION AND VELOCITY MEASUREMENTS  
IN THE SEPARATED REGION OF AN APPENDAGE-  
FLAT PLATE JUNCTION

Stuart C. Dickinson  
David W. Taylor Naval Ship  
Research & Development Center  
Bethesda, Maryland 20084

ABSTRACT

A "root" vortex forms at the junction of a flat plate and an appendage, creating a three-dimensional, separated flow. Time dependent oil film and oil dot visualizations of this turbulent flow have revealed the vortex system and have provided quantitative information on the direction and the magnitude of the shear stress. Two-dimensional LDV mean velocity measurements were made in the separated flow region around the leading edge of the appendage, and these measurements are compared here with the flow visualization results.

INTRODUCTION

The junction between a body and an appendage is a simple configuration with a complicated flow. Such configurations are found in many areas of fluid engineering including the wing-fuselage junction of aircraft, the appendage-hull junction of ships, and the blade-shroud junction of turbomachinery. The "root" vortex secondary flow affects the drag, lift, and heat transfer in the junction, and causes a persistent lack of uniformity in the wake. A good review of such flows is found in Peake and Tobak (1980). The work presented here is part of a large scale effort to understand and document an idealized appendage-body junction flow in order to assist in developing accurate numerical flow prediction codes for naval designs.

In a simple description of the vortex

formation, the vorticity present in the oncoming body boundary layer is slowed down by the pressure gradients near the leading edge of the appendage. Away from the junction, the flow continues undisturbed so the vorticity is wrapped around the appendage. A concentration and a turning of the oncoming cross-stream vorticity into streamwise vorticity occurs. The result is a horseshoe root vortex secondary flow with three dimensional separations and attachments.

Oil film and oil dot flow visualization techniques are common ways to determine surface separation and attachment lines, as well as wall streamline patterns. Time lapse photography was also used to study the development of the visualization and infer a qualitative picture of the surface shear stress. Two dimensional LDV measurements were made in the separated flow regions, and these are used in conjunction with the flow visualization to describe parts of the "root" vortex secondary flow.

EXPERIMENTAL DESCRIPTION

These experiments were performed in the David Taylor Naval Ship Research and Development Center (DTNSRDC) Low Turbulence Wind Tunnel. The test section is 0.61 m wide (2 ft), 1.22 m high (4 ft) and 4.57 m long (15 ft). The test section velocity is variable up to 40 m/sec (130 ft/sec) with a free stream turbulence level less than 0.2%. Access to the test section is through the top. This surface is used as the flat plate of the appendage junction. The appendage is

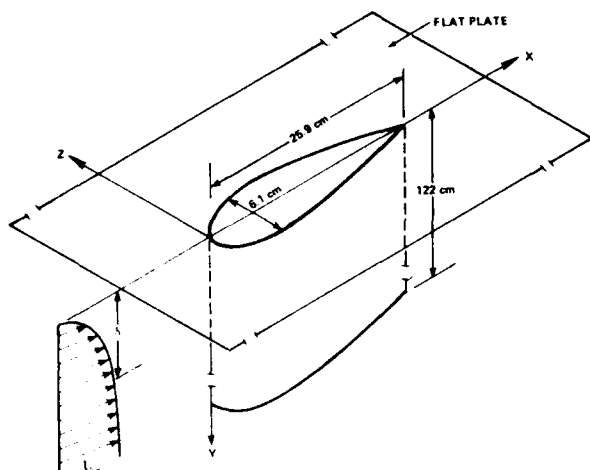


Figure 1. Appendage junction coordinate system and configuration.

semi-infinite, spanning the height of the tunnel. The foil shape is a hybrid consisting of a 1.5:1 elliptical nose and a NACA 0020 tail joined at the locations of maximum thickness. The resulting appendage has a chord of 25.9 cm and a thickness of 6.1 cm (see Figure 1). A right-handed cartesian coordinate system is used with the origin at the leading edge junction, and with the X-axis positive in the downstream direction (see Figure 1). The leading edge of the foil is centered in the tunnel 3.5 m (11.5 ft) from the entrance of the test section. The flat plate (tunnel roof) velocity boundary layer thickness  $\delta$  at this position is 4.7 cm (1.85 in) without the appendage, and at the nominal test velocity  $U_\infty = 34$  m/sec. The velocity profile agrees well with the  $1/7$  power law of a self-similar turbulent boundary layer. This results in a calculated momentum thickness  $\theta = (7/12) \delta = 0.46$  cm (Schlichting 1979) and a boundary layer Reynolds number  $R_\theta \approx 9,800$ .

The appendage has a cylindrical trip wire 0.33 mm in diameter located at 5% of chord in order to ensure turbulent flow. The foil was always maintained at zero degrees angle of attack as determined by a pair of static pressure taps and wake surveys. A plexiglass window 0.46 m by 0.79 m inset flush in the tunnel roof allowed photographic and LDV access to the flow.

Static pressure measurements were made on the flat plate in the vicinity of the appendage (Figure 2). These pressures agree well with those calculated for a potential flow, with some variations due to the secondary flow velocities.

## FLOW VISUALIZATION

### Oil Films

Surface flow patterns can be revealed by use of oil film techniques. Traditional methods examine an oil pigment mixture which has run to "completion", i.e., the pattern left after the oil has either evaporated or stopped moving. The assumption is made that the pigment streaks left behind closely follow the air surface streamlines (Merzkirch 1974). Steady separation lines are easily seen as oil-pigment accumulations, and attachment lines may be seen either as areas free of pigment or as the source of streamlines. Time dependent oil film flow visualization uses several views of the film as the flow pattern develops. During this process, the oil is moving at a speed and direction proportional to the local shear stress. In a flow like the appendage flat plate junction, the shear stress varies from place to place. Using photographs of the oil film at known time intervals, one can qualitatively determine relative shear stresses. Figure 3, A-F shows the flow pattern at various times  $T$  after the wind tunnel has rapidly been brought up to speed.

Frame A shows the film for  $T=0$ . At  $T=0.5$  min, Frame B, the oil has been removed from the area next to the leading edge, revealing the area of highest shear stress. Frame C ( $T=1$  min) shows the clear area moving upstream and lengthening around the foil. The oil has been scoured to the inner line in Frame D ( $T=4$  min) and is starting to move between this line and the primary separation. The outer region ("potential flow" area) and the downwash area aft of the tail have also started to develop patterns. The clear lines close to and alongside the foil reveal a counter-rotating "inner" vortex with the oil collecting in the corner. In Frame E ( $T=10$  min) the tail area pattern has developed and the leading edge region has "completed" or lost its oil. This frame shows a problem with using

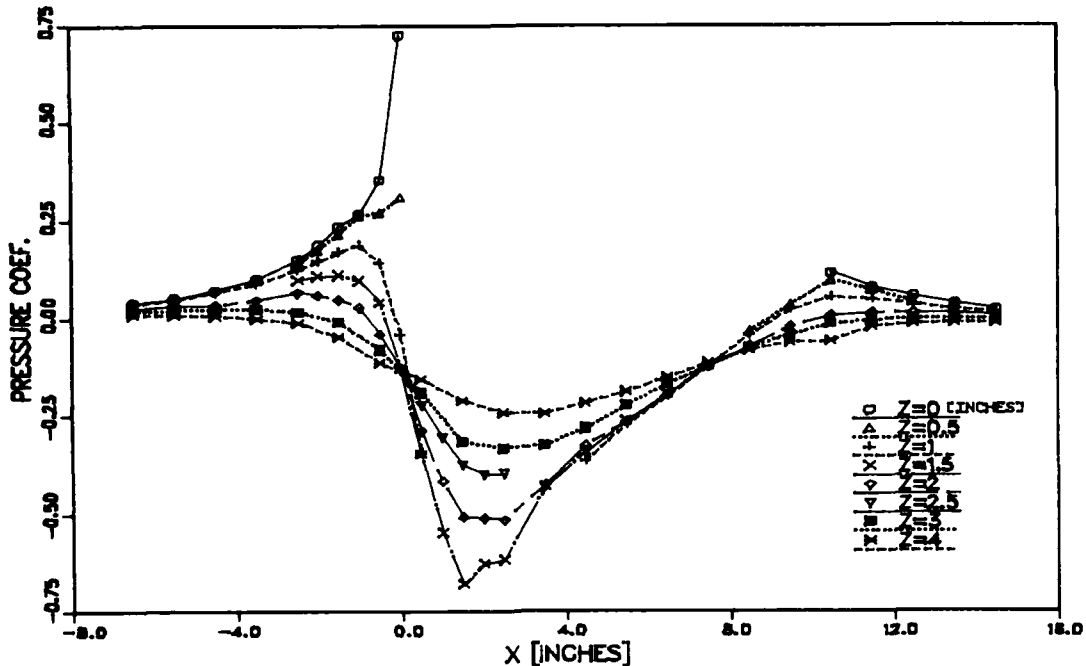


Figure 2. Static pressure coefficients  $P_s/(1/2\rho U_\infty^2)$  measured on the flat plate.

this technique for large areas: The oil scoured from the upstream areas has flowed into the tail region creating a thick film and obscuring the true patterns locally. After 40 minutes, Frame F shows the completed picture of the traditional method.

Figure 4 is a sketch of the fully developed oil film pattern. It shows the primary separation line wrapped around the leading edge and trailing downstream. There is an inner line in the leading edge region which merges with the primary separation near the one-half chord position. This line is interpreted not as a separation line but as a sharp demonstration between a high shear stress region inside and a much lower shear stress region outside. An attachment line is shown which is between a small inner counter-rotating vortex and the primary "root" vortex. In the tail region, the vortex induces a downwash, and "Y" shaped separation lines are observed.

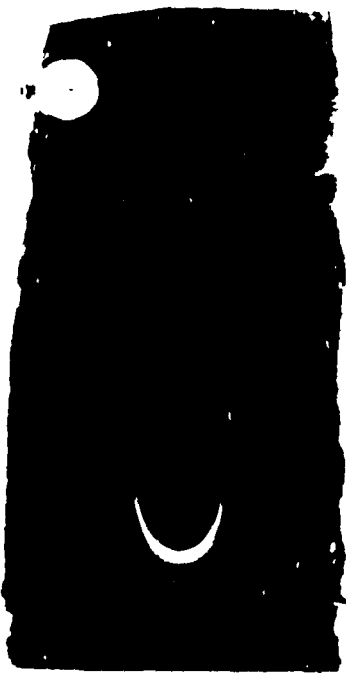
#### Oil Dots

Oil dot flow visualization is typically used to show the surface streamline pattern. The oil dot streaks are moving material lines with the downstream "head" as the source of the line. The length of the line will be proportional to the

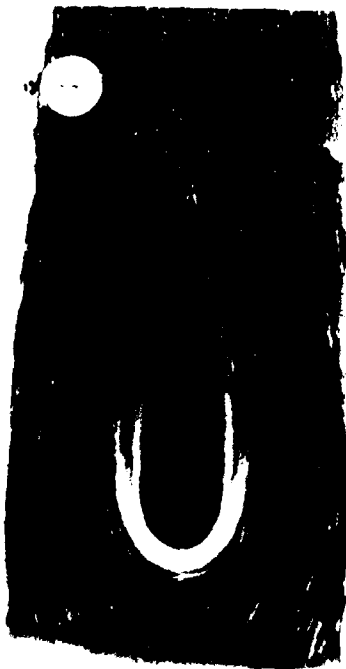
shear stress if three conditions are met. First, the initial volume of the drops must be constant; second, the "head" must not be depleted of oil; and third, the length must be measured at the same time.

Three forces have been identified as possible sources of error: gravity, surface tension, and static electricity. Gravity can be controlled by making the surface as near horizontal as possible. Surface tension needs to be uniform over the body, and this can be achieved by proper surface preparation. If, however, the shear stress is not large enough, the oil drop will not move because of the surface tension forces. The static electricity which builds up during the cleaning of glass and plastic surfaces can be reduced with a conductive spray (commercially available for use on clothing).

Figure 5 is a composite of five runs with oil dots. The circles represent the initial placement of the oil. The line is the center of the resulting streak. Care was taken to prevent the streaks from running to completion. Five runs were used to keep the streaks from running into each other and to reduce the spreading of the drops during the application process.



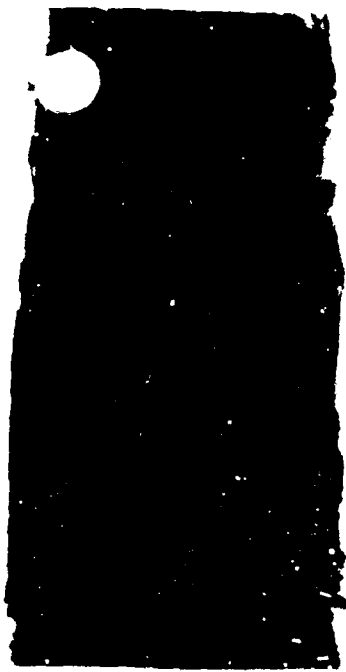
B



D



E



A



C



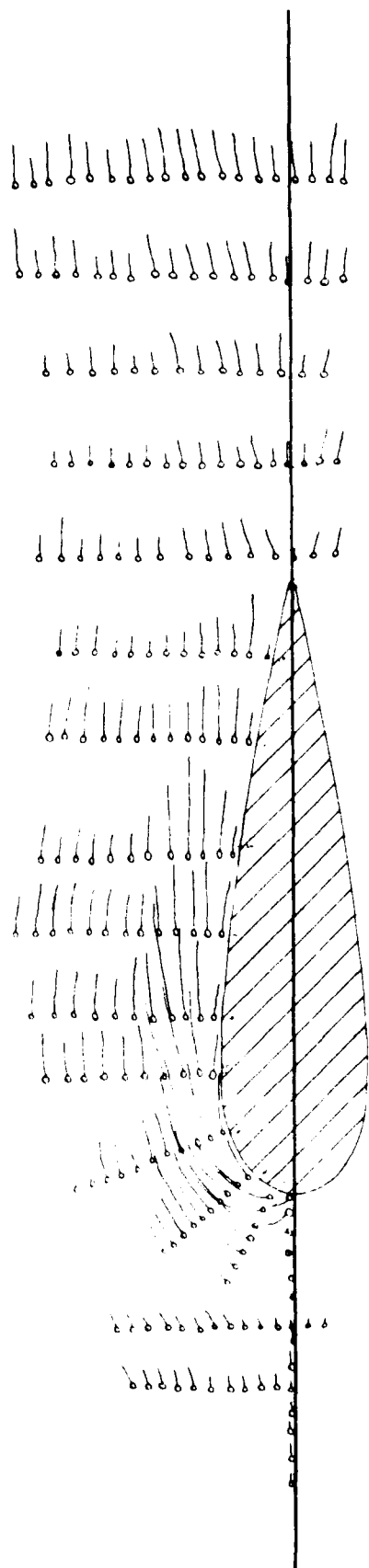


Figure 5. Oil dot visualization pattern.

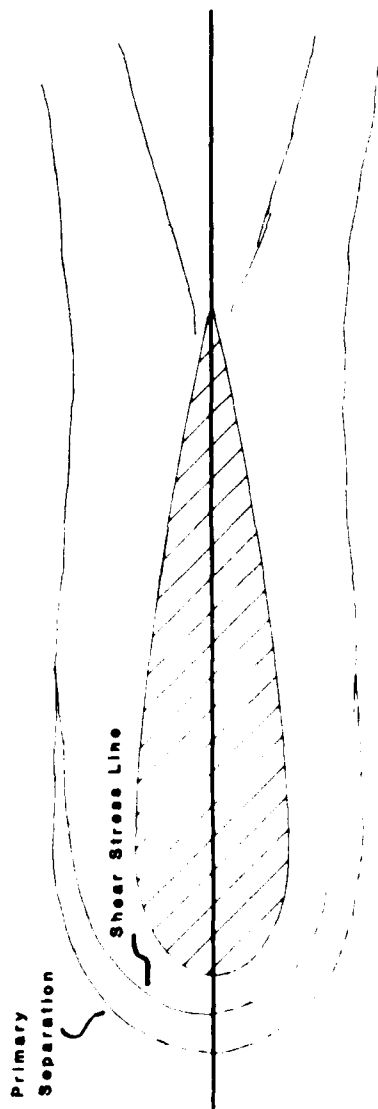


Figure 4. Sketch of "completed" oil film visualization.

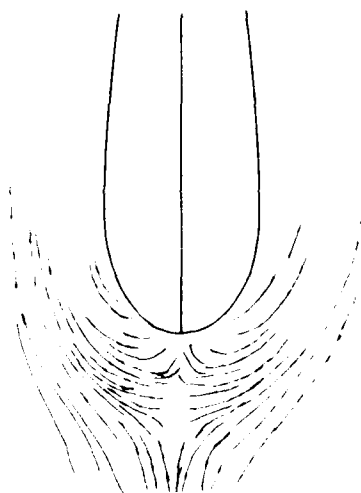


Figure 6. Sketch of oil of wintergreen visualization.

A screw-actuated hypodermic was used to produce reasonably uniform drop volumes on the ceiling of the wind tunnel. The length of the streak lines should be proportional to the shear stress along each row of dots.

Essential features of the flow highlighted by this oil dot technique are seen in Figure 5. A low shear stress region is seen near the leading edge separation. The forward moving reversed flow is clearly seen near the center line, just forward of the appendage. As the flow accelerates around the elliptical nose, the vortex induces outward flow and high shear stress is apparent. Along the side of the appendage, the primary separation can be observed as a convergence of the streamlines. The small, inner, counter-rotating vortex is shown by the dots along the junction (rows 3-7) moving in toward the appendage and by the divergence of streamlines between the first and second sets of dots. Row 8 is the clearest example of the variation of shear stress in the cross-stream plane. Moving out from the appendage, the stress increases under the core of the vortex; then the stress reaches a minimum near the separation line and finally, it becomes constant in the outer region. In the wake region, the downwash is seen via the divergence. Along the wake centerline the shear stress increases downstream as the wake velocity deficit (downwashed to the wall) is reduced.

Comparisons between Figures 4 and 5 show good agreement between these two flow visualization techniques. A close examination was made of the leading edge region using the oil of wintergreen technique (Langston & Boyle (1982)). A sketch of the results is seen in Figure 6. Streamlines cross the shear stress gradient line of Figure 4, indicating that this appendage junction flow has a single root vortex.

#### LDV MEASUREMENTS

A two-component LDV system was used to take mean velocity measurements in the vicinity of the appendage flat plate junction. Reversed flow could be detected in the separated region near the appendage leading edge through the use of a

frequency shifted system. The hardware used was a two-component, two-color system utilizing four beams, manufactured by TSI, Inc. Frequency shift was available on both channels. A 150 mm diameter, 1200 mm focal length objective lens was used to produce the beam crossing. The receiving optics were the on-axis backscatter type. A TSI Model 1990 counter processor was used. The counter output was interfaced to a PDP-1123 computer and the data was processed with TSI, Inc. software.

Seed particles consisted of Huber-70C Kaolin Clay with an average particle diameter of 1.5  $\mu\text{m}$  and a specific gravity of 2.63. These were sprayed in an alcohol-clay mixture upstream of the wind tunnel screens and settling chamber. The alcohol (ethanol) evaporated leaving the clay seed particles.

The 0.5145  $\mu\text{m}$  green line and the 0.488  $\mu\text{m}$  blue line of an ion-argon laser were used for the two color system. With a 140 mm beam spacing, the beam half angle was nominally 3.34°. The measurement volume was approximately 3.6 mm long along the optical axis and 0.21 mm in diameter. The green beams were used for the streamwise (U) velocity and the blue beams for the horizontal cross-stream (W) velocity. The blue beams were operated with a 5 MHz frequency shift to ensure at least 16 fringe crossings when a streamwise moving particle traversed the probe volume. The green beams were frequency shifted as necessary in the separated flow regions. Due to restricted access in the wind tunnel, the beams were reflected off a 45° angled mirror, and entered the flow field along the vertical (Y) axis (see Figure 7). A "super abrasion resistant" plexiglass window 1/2 inch (1.25 cm) thick was used. This window was the flat plate of the appendage junction. The plexiglass caused reflection-induced signal-to-noise problems when operating less than 1 cm from the surface with frequency shifted beams. This problem was overcome for the streamwise component by angling the optical axis approximately 3.5° off normal incidence. Using angled beams, streamwise velocities could be obtained as close as 2.5 mm (position of the center of the probe volume) from the window.

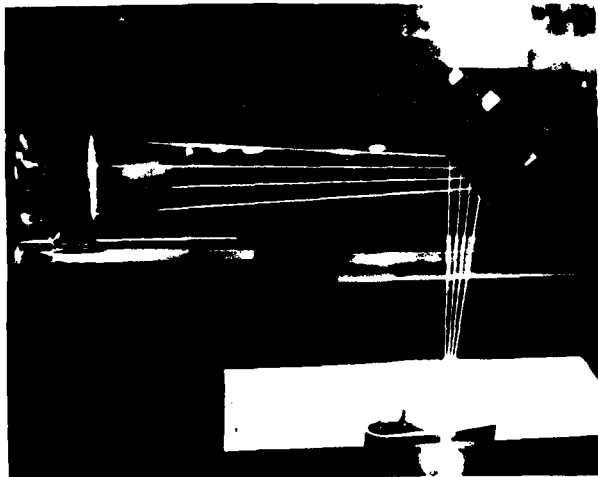


Figure 7. Photograph of LDV beam configuration.

LDV velocity measurements were taken as flat plate boundary layer profiles in five measurement planes.  $U$  and  $W$  mean velocities were measured at  $X = \text{constant}$  planes 16.5 and 1.65 cm ahead of the appendage and at 2.54 cm and 16.5 cm alongside of the appendage. Streamwise ( $U$ ) mean velocities were also measured on the plane of symmetry ( $Z=0$ ) ahead of the appendage using angled beams. The velocity errors were estimated to be  $\pm 1\%$  of freestream outside of the boundary layer increasing to  $\pm 5\%$  of freestream at distances less than a centimeter from the flat plate.

Figure 8 shows the velocities approximately 60% of a chord length upstream of the appendage. The flow is similar to a normal turbulent boundary layer, but the effect of the appendage can be seen. Figure 9 shows the velocities in a plane just ahead of the foil. The outer flow is in the potential flow, with the streamwise velocity ( $U$ ) increasing with cross-stream ( $Z$ ) distance, and the cross-stream velocity  $W$  going through a maximum and decreasing as the streamlines straighten away from the appendage. At a distance of about  $\delta$  from the wall, a slight increase in streamwise velocity is seen in the area ahead of the foil. A slight inflow (relative to outside the boundary layer) is seen in the  $W$  velocity profiles at distances the order of the appendage half-thickness from the centerline. Just aft of the leading edge (Figure 10) the measured

velocities reflect the flow acceleration around the appendage. The constant  $W$  velocity profiles indicate a rotation of the velocity vector through the outer portions of the boundary layer.

Figure 11 represents the velocities at approximately 60% of chord. The streamwise velocity profiles show several interesting features. In the outer region, the appendage boundary layer can be seen. A strong maximum can be seen in the two inner profiles ( $z = 0.8, 0.825$  in), indicating an inflow of higher velocity fluid. The ( $z = 1.0, 1.25$  in) profiles show less curvature near the flat plate, demonstrating influx of higher speed fluid. The cross-stream velocities ( $W$ ) do not exhibit any strong tendencies. The inner profiles are truncated, however, due to laser beam blockage by the model.

Figure 12 shows streamwise velocities ahead of the foil along the axis of symmetry. These profiles were measured using angled beams allowing closer access to the flat plate. The deceleration of the flow approaching the appendage leading edge is apparent. The lack of negative mean velocities near the junction is of particular interest.

#### DISCUSSION

An appendage flat plate junction has a complex "root" vortex secondary flow. Flow visualization and velocity measurements have been made to reveal some of the essential features of this flow.

Oil film flow visualization studies show a significant three dimensional separated zone. This zone, caused by the vortex secondary flow, is wrapped around the appendage and trails off downstream. Time dependent oil film techniques reveal large differences in surface shear stress on the flat plate with the high stress zones indicating the location of the vortex flow. Oil dot flow visualizations clearly show the upstream reversed flow near the leading edge and the outwardly directed surface streamlines under the vortex alongside of the appendage.

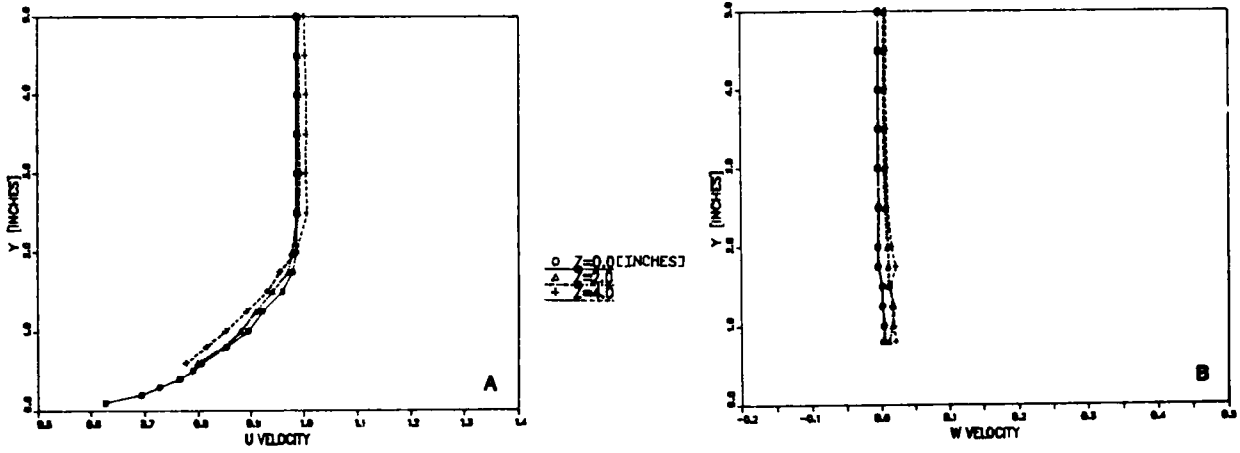


Figure 8. Normalized U and W velocity profiles at X = -6.5 in. (upstream).

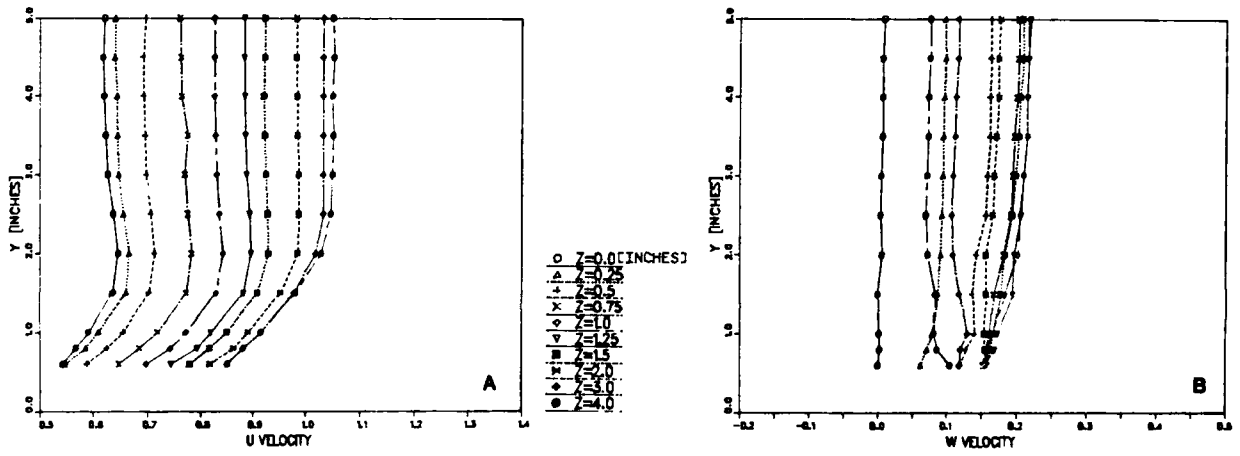


Figure 9. Normalized U and W velocity profiles at X = -0.65 in. (just ahead of the appendage).

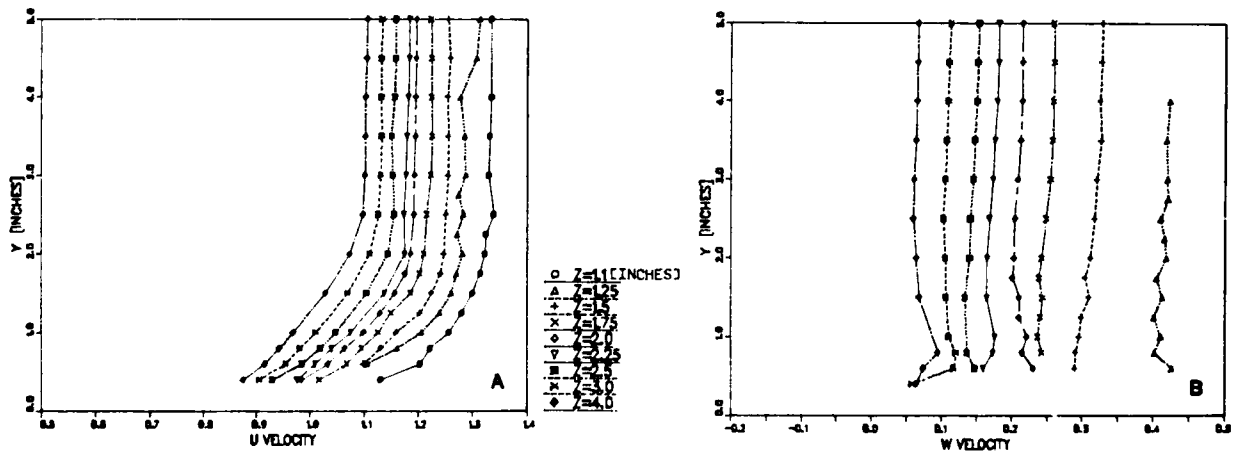
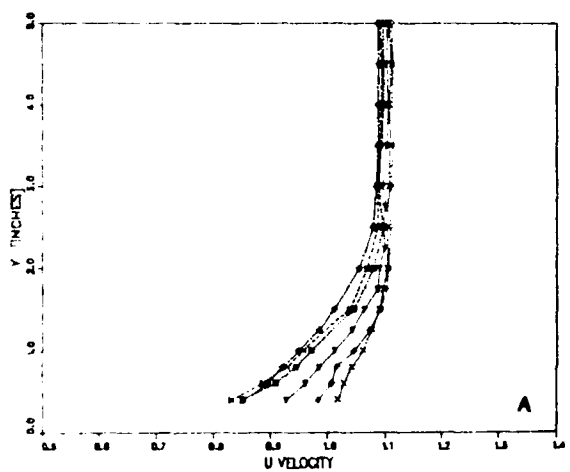
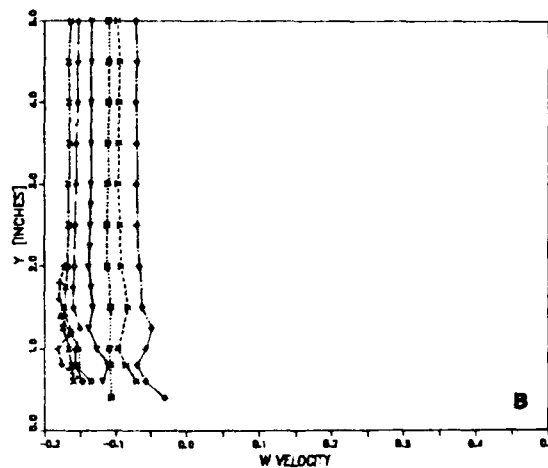
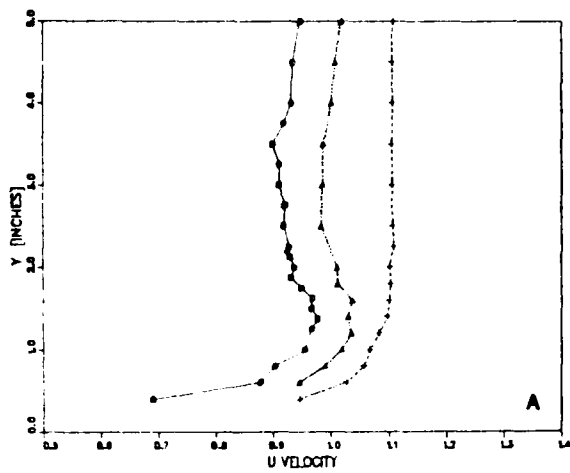
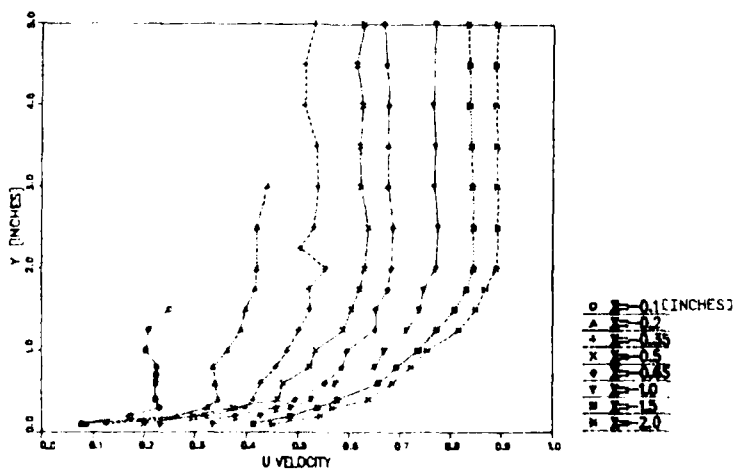


Figure 10. Normalized U and W velocity profiles at X = 1.0 in.



○ Z=0.8 [INCHES]  
 ▲ Z=0.875  
 × Z=0.9  
 ◆ Z=0.95  
 ▼ Z=1.0  
 ■ Z=1.5  
 □ Z=2.0  
 ● Z=4.0

Figure 11. Normalized U and W velocity profiles at X = 6.5 in. Figure A shows the appendage boundary-layer (upper graph) separately for clarity.



○ X=0.1 [INCHES]  
 ▲ X=0.2  
 × X=0.3  
 ◆ X=0.4  
 ▼ X=0.5  
 ■ X=0.6  
 □ X=0.7  
 ● X=0.8

Figure 12. Normalized U velocity profiles along the plane of symmetry (Z=0) ahead of the appendage.

Laser Doppler Velocimeter measurements made in the separation region show effects of pressure driven flows. Outside of the flat plate turbulent boundary layer, potential flow was seen. Traversing through the boundary layer a pressure driven skewing of the velocity was seen. However, even though measurements were made close to the wall, the mean reversed and strong cross-stream flows of the expected vortex were not observed.

To reconcile the flow visualization results with the velocity measurements, the vortex must have small dimensions (of order of the momentum boundary thickness) in the direction normal to the flat plate. This conclusion is supported by the reversed flows observed in the LDV velocity histograms near the leading edge and in reversed flow sensing hot wire measurements by McMahon et al. (1983). The flow visualizations show that the primary separation line (on the flat plate) occurs approximately 1/2 of the appendage thickness away from the junction. This implies that the "root" vortex is flattened like a "tank track" in the forward region of the appendage. Downstream along the aft portions of the appendage and in the wake, one would expect the vortex to move up in the boundary layer and become "rounded". Velocity measurements by Shabaka (1979) shows this smoothing and lifting for an infinitely long parallel-aided appendage. The oil dot streak lengths show the reduction in shear stress downstream that would accompany the upward movement of the vortex.

#### ACKNOWLEDGEMENTS

This work was supported by the Navy Sea Systems Command under the Ship and Submarine Appendage Drag and Wake Prediction Special Focus Program. The author appreciates the assistance of Mr. R. David Middlekauff during the LDV phase of the work.

#### REFERENCES

- Langston, L.S., and Boyle, M.T., 1982, "A New Surface-Streamline Flow-Visualization Technique", *J. Fluid Mech.*, 125, pp.53-57.
- McMahon, H., Hubbartt, J., and Kubendran, L.R., 1983, "Mean Velocities and Reynolds Stresses Upstream of a Simulated Wing-Fuselage Junction", NASA Contractor Report 3695.
- Merzkirch, W., 1974, Flow Visualization, Academic Press, New York.
- Peake, D.J., and Tobak, M., 1980, "Three-Dimensional Interactions and Vortical Flows With Emphasis on High Speeds", AGARDograph No. 252.
- Schlichting, H., 1979, Boundary-Layer Theory (Seventh Edition), McGraw-Hill Book Co., New York, p. 638.
- Shabaka, I.M.M.A., 1979, "Turbulent Flow in an Idealized Wing-Body Junction", PhD. Thesis, Imperial College of Science and Technology.

INITIAL DISTRIBUTION

Copies		Copies	
2	ONR 1 1132F (C. Lee) 1 1132F (M. Reischman)	4	Pennsylvania State University 1 Merkle 1 Parkin 1 Hoffman 1 ARL-Lib
3	NAVSEA 1 SEA 05R (F. Ventriglio) 1 SEA 55W31 (W. Sandberg) 1 SEA 55W31 (C. Chen)	1	Univ. of Southern California Eibeck
2	NBS 1 Klebanoff 1 Lib	1	Rutgers Univ. Knight
2	NASA, Langley 1 Kubendran 1 Lib	2	Univ. of Iowa 1 Patel 1 Stern
2	NASA, Ames 1 Kwak 1 Lib	5	Stevens Institute of Tech. 1 Speziale 1 Savitsky 1 Breslin 1 McKee 1 Davidson Laboratory- Lib
2	Flow Research Co. 1 Duncan Silver Spring, MD 1 Gad-el-Hack Kent, WA	1	New Jersey Institute of Tech. Battifarano
1	Gould Defense Systems, Inc. Meng	3	Scientific Research Assoc., Inc. 1 Levy 1 Shamroth 1 Briley
1	Massachusetts Institute of Tech., Merrill	1	Lockheed Georgia Co. Thomas
1	Univ. of Southern Calif, Ho		
4	Virginia Poly, Inst. & State Univ 1 Pierce 1 Moore 1 Shetz 1 Simpson	12	DTIC
2	Georgia Institute of Tech. 1 Hubbartt 1 McMahon		

CENTER DISTRIBUTION

Copies	Code	Name
1	012.2	Nakonechney
1	15	Morgan
1	1504	Monacella
1	152	Lin
1	1522	Sung
1	154	McCarthy
1	1542	Huang
25	1542	Dickinson
1	1542	Burke
1	1543	Rood
1	1543	Anthony
1	1544	Peterson
1	1544	Reed
1	1843	Hausling
10	5211.1	Reports Distribution
1	522.1	TIC (C) + 1m
1	522.2	TIC (A)

**DTICRDC ISSUES THREE TYPES OF REPORTS:**

- 1. DTICRDC REPORTS, A FORMAL SERIES, CONTAIN INFORMATION OF SIGNIFICANT TECHNICAL VALUE. THEY CARRY A CONSECUTIVE NUMERICAL IDENTIFICATION SYSTEM AND THEIR CLASSIFICATION OF THE ORIGINATING DEPARTMENT.**
- 2. DEPARTMENTAL REPORTS, A SEMI-FORMAL SERIES, CONTAIN INFORMATION OF A GENERAL, INQUIRY, TEMPORARY, OR PROPRIETARY NATURE OF LIMITED INTEREST OR IMPORTANCE. THEY CARRY A DEPARTMENTAL ALPHANUMERICAL IDENTIFICATION.**
- 3. TECHNICAL MEMORANDA, AN INFORMAL SERIES, CONTAIN TECHNICAL INFORMATION OF LIMITED USE AND INTEREST. THEY ARE PRIMARILY DESIGNED FOR INTERNAL USE. THEY CARRY AN IDENTIFYING NUMBER WHICH INDICATES THEIR TYPE AND THE NUMERICAL CODE OF THE ORIGINATING DEPARTMENT. ANY DISTRIBUTION OUTSIDE DTICRDC MUST BE APPROVED BY THE HEAD OF THE ORIGINATING DEPARTMENT ON A CASE-BY-CASE BASIS.**

END

FILMED

6-86

DITIC